

# Transition Metal Doped MnO<sub>x</sub>-CeO<sub>2</sub> Catalysts by Ultrasonic Immersing for Selective Catalytic Reduction of NO with NH<sub>3</sub> at Low Temperature

Jinshuo Qiao<sup>1</sup>, Ning Wang<sup>1</sup>, Cuiya Zhuang<sup>1</sup>, Kening Sun<sup>2\*</sup>

<sup>1</sup>Beijing Key Laboratory for Chemical Power Source and Green Catalysis, School of Chemical Engineering and the Environment, Beijing Institute of Technology, Beijing, China

<sup>2</sup>Academy of Fundamental and Interdisciplinary Sciences, Harbin Institute of Technology, Heilongjiang, China  
Email: \*[keningsunhit@126.com](mailto:keningsunhit@126.com), [qjinshuo@bit.edu.cn](mailto:qjinshuo@bit.edu.cn)

Received 21 October 2014; revised 22 November 2014; accepted 21 December 2014

Copyright © 2015 by authors and Scientific Research Publishing Inc.

This work is licensed under the Creative Commons Attribution International License (CC BY).

<http://creativecommons.org/licenses/by/4.0/>



Open Access

---

## Abstract

Transition metals doped Mn-based catalysts were prepared via ultrasonic immersing method for the selective catalytic reduction (SCR) of NO<sub>x</sub> from fuel gas. The Catalysts' DeNO<sub>x</sub> efficiency and tolerance to sulfur were investigated in the paper. XRD results demonstrate high dispersion of Mn, Ce and M (Pr, Y, Zr, W) elements on TiO<sub>2</sub> carrier, which is favor for reduction of active materials content. Mn-Ce-W catalyst presents uniform particle size about 500 nm to 800 nm from SEM pictures and shows the best NO<sub>x</sub> conversion of 93.2% at 200°C and 98.4% at 250°C, respectively. Sulfur tolerance analysis indicated that transition metals M can improve the catalysts' performance when 0.01% SO<sub>2</sub> exists in the fuel gas, because metal doping into the Mn-Ce catalyst can inhibit the sulfate deposition, especially metal sulfate, on the catalyst, which can be seen from the Fourier infrared spectrum.

## Keywords

Mn-Based Catalysts, Ultrasonic Immersing Method, Selective Catalytic Reduction, Sulfur Tolerance

---

## 1. Introduction

Strict control of NO<sub>x</sub> emission is urgently needed due to the increasing effect on the environment from urban

---

\*Corresponding author.

smog, ozone depletion and greenhouse. The selective catalytic reduction (SCR) technology with  $\text{NH}_3$  is considered as the most effective method to remove  $\text{NO}_x$  in flues gases. The SCR catalysts have been developed in the past decades and Vanadium-based catalyst is the commercial one for application at temperature  $300^\circ\text{C}$  -  $400^\circ\text{C}$  due to its high  $\text{DeNO}_x$  efficiency and good sulfur-resistance. However, these catalysts show the toxicity of raw materials and high cost, which limit their extensive applications. So developing catalysts working less than  $300^\circ\text{C}$  is of interest due to their possible application in downstream after desulfurizer and electrostatic. Various catalysts have been investigated at low temperature such as Manganese oxides ( $\text{MnO}_x$ ) supported on  $\text{Al}_2\text{O}_3$ ,  $\text{TiO}_2$  and  $\text{SiO}_2$ . The results show that  $\text{MnO}_x$  is a kind of promising catalyst applied at low temperature. At the same time, ceria is found to increase the oxygen storage capability of  $\text{MnO}_x$  and enhance the migration rate of oxygen. In present,  $\text{MnO}_x$ - $\text{CeO}_2$  catalysts have been demonstrated possessing the high  $\text{NO}_x$  removal efficiencies [1]-[4]. However,  $\text{MnO}_x$ - $\text{CeO}_2$  catalysts have no ideal sulfur-resistance with a long time, especially under the co-existence of  $\text{H}_2\text{O}$  and  $\text{SO}_2$  [5] [6].

In this work, transition metals will be doped into Mn-based catalysts to improve the catalyst's tolerance to sulfur. Then ultrasonic immersing method was used to prepare catalysts, which apparently reduce the preparation period comparing to sol-gel method. The transition metals effect on  $\text{DeNO}_x$  efficiency and sulfur tolerance of catalysts was discussed in details as following.

## 2. Experimental Section

### 2.1. Catalyst Synthesis

The  $\text{TiO}_2$  powder (Industrial grade, 96% purity, 15 - 25 nm,  $93.9 \text{ m}^2 \cdot \text{g}^{-1}$ ) was dried at  $105^\circ\text{C}$  for 1 h and milled for 150 mesh. Manganese nitrate, cerium nitrate and nitrate of transition metal (M) (Sinopharm Chemical Reagent Co.) at a certain ratio are solved into Deionized water (DW). Then, the obtained solution was placed into the ultrasonic reaction pool. The processed  $\text{TiO}_2$  powder was added into the solution when the metal nitrate dissolved fully under the stirring condition with 160 W ultrasonic at  $50^\circ\text{C}$  for 24 h. Then the immersed  $\text{TiO}_2$  powder was dried at  $105^\circ\text{C}$  for 24 h, calcined at  $450^\circ\text{C}$  for 6 h and milled for 150 mesh to obtain catalysts powder. The obtained catalyst was expressed as  $\text{Mn-Ce-M}_{0.025}$ , and M represent W, La, Pr and Zr. The mole ratio of  $\text{Ti}:\text{Mn}:\text{Ce}:\text{M}$  is 1:0.4:0.07:0.025.

### 2.2. Catalyst Characterization

The catalyst's catalytic activity was measured in a quartz reactor (35 cm i.d.) using 6.75 g catalyst, see in **Figure 1**. The feed gas mixture in a  $\text{N}_2$  stream contained 1000 ppm  $\text{NO}$ , 1100 ppm  $\text{NH}_3$ , and 5%  $\text{O}_2$ . The total flow rate of the feed gas was 90 L/h ( $\text{GHSV} = 10,000 \text{ h}^{-1}$ ). The reaction temperature was scanned from  $100^\circ\text{C}$  to  $400^\circ\text{C}$ .

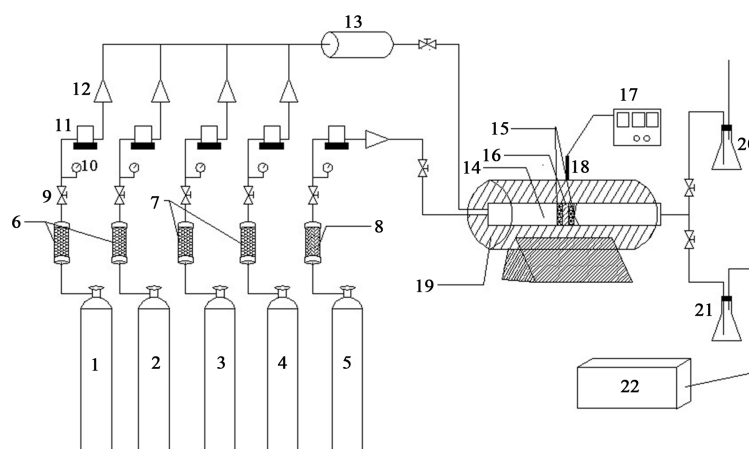


**Figure 1.** Experimental setting and flow chart. 1— $\text{N}_2$ ; 2— $\text{O}_2$ ; 3— $\text{SO}_2$ ; 4— $\text{NO}$ ; 5— $\text{NH}_3$ ; 6—Silica gel drying apparatus; 7— $\text{CaCl}_2$  dryer; 8— $\text{CaO}$  dryer; 9—Stop valve; 10—pressure gage; 11—mass flow meter; 12—one-way valve; 13—mixer; 14—quartz tube; 15—silica wool; 16—catalysts; 17—temperature control for furnace; 18—thermocouple; 19—tube furnace; 20— $\text{NaOH}$  washing bottle; 21— $\text{H}_3\text{PO}_4$  washing bottle; 22—flue gas analyzer.

The concentration of the  $\text{NO}_x$  in the inlet and outlet of the reactor were measured on-line by a flue gas analyzer (MRU, Germany).  $\text{H}_2$ -temperature-programmed reduction ( $\text{H}_2$ -TPR, ChemBET Pulsar) experiments were carried out using every catalyst (40 mg) under a mixed gas flow of  $\text{H}_2$  and Ar. Morphologies of the samples were characterized by scanning electron microscopy (SEM, quanta FEG 250). Powder XRD was characterized with Cu-K $\alpha$  radiation at the range of  $10^\circ$  -  $90^\circ$ . Fourier infrared spectrum (FT-IR, Prestige-21) was used to analyze functional group change of catalyst after operating for a time.

### 3. Results and Discussion

#### 3.1. Structure and Morphology Analysis

XRD patterns of the Mn-Ce-M catalysts are shown in **Figure 2**. Only  $\text{TiO}_2$  peaks in all catalysts suggests a low loading and a high dispersion of Mn, Te and M elements on the surface of  $\text{TiO}_2$ . At the same time, compared with pure  $\text{TiO}_2$  (industrial grade), the  $\text{TiO}_2$  peaks become weak for all the catalyst, which further shows uniform active ingredients with small size for the catalyst can be obtained by impregnation technology. **Figure 3** gives the SEM pictures of Mn-Ce-M catalyst. W-doped catalyst reveals uniform particle size from 500 nm to 800 nm as same as Mn-Ce catalyst. Adding Pr into Mn-Ce catalyst lead to slightly agglomeration of the catalyst particle, see the **Figure 3(c)**. The prepared Mn-Ce-Zr and Mn-Ce-Y catalysts show obvious particle agglomeration, in the **Figure 3(d)** and **Figure 3(e)**. At the same time, metal doping lead to bulk density increase or the porosity decrease of the catalyst. The catalyst morphology may possibly influence its performance, which need be investigated in the following.

#### 3.2. Catalyst Performance

The catalytic performance of Mn-Ce- $\text{M}_{0.025}$  catalysts, expressed as the percent conversion of NO as function of temperature, is shown in **Figure 4**. The Mn-Ce catalyst behaves above 80% NO conversion at  $150^\circ\text{C}$  -  $300^\circ\text{C}$  and achieved the maximum value with 91% conversion at  $200^\circ\text{C}$ . Compared with Mn-Ce catalyst, Mn-Ce-M catalyst presents the lower NO conversion at  $100^\circ\text{C}$  -  $150^\circ\text{C}$ . Above  $200^\circ\text{C}$ , the Mn-Ce-W catalyst shows the most excellent performance and obtains the 93.2% and 98.4% NO conversion at  $200^\circ\text{C}$  and  $250^\circ\text{C}$  respectively. Pr elements doped Mn-Ce catalysts decrease the catalytic performance relative to Mn-Ce catalyst at all test temperature. At the same time, Zr and Y elements addition into the Mn-Ce catalyst reduce the lower-temperature ( $100^\circ\text{C}$  -  $200^\circ\text{C}$ ) performance and enhanced NO conversion at the high temperature ( $300^\circ\text{C}$  -  $400^\circ\text{C}$ ). At  $250^\circ\text{C}$ , the Mn-Ce-Zr catalyst with 92.2% NO conversion is higher than that of Mn-Ce catalyst. The performance of Mn-Ce-Y catalyst is near to that of Mn-Ce catalyst. These results demonstrate W element efficiently improves the catalyst's NO conversion and Pr element presents poor action. Zr and Y elements promote Mn-Ce

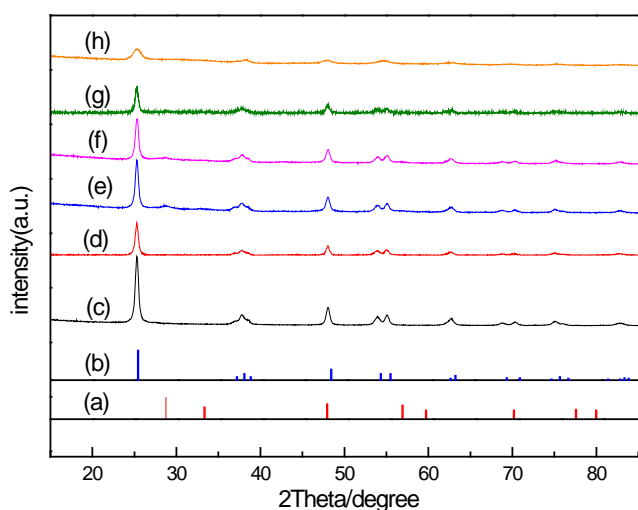


**Figure 2.** XRD patterns of I-Mn-Ce-M. (a)  $\text{CeO}_2$  standard PDF#34-0394; (b)  $\text{TiO}_2$  standard-PDF#21-1272; (c) Industrial-grade  $\text{TiO}_2$ ; (d) Mn-Ce; (e) Mn-Ce-W; (f) Mn-Ce-Pr; (g) Mn-Ce-Zr; (h) Mn-Ce-Y.

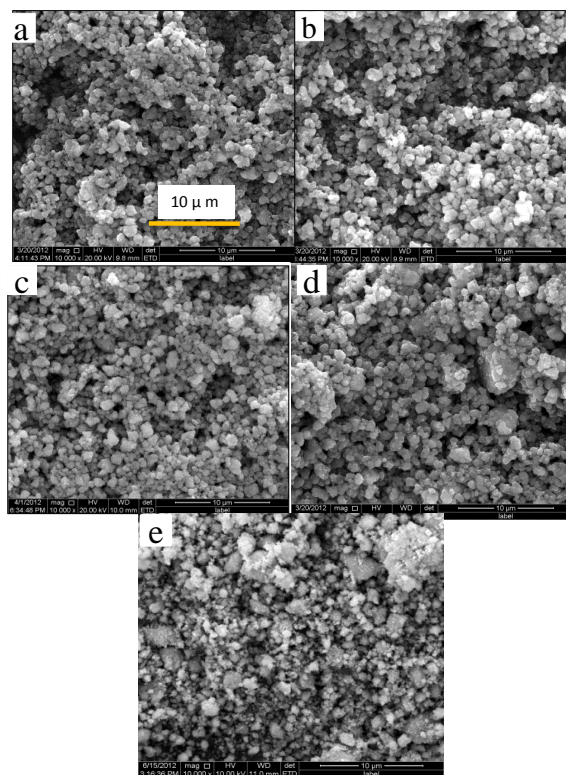


**Figure 3.** SEM micrographs of Mn-Ce-M. (a) Mn-Ce; (b) Mn-Ce-W; (c) Mn-Ce-Pr; (d) Mn-Ce-Zr; (e) Mn-Ce-Y.

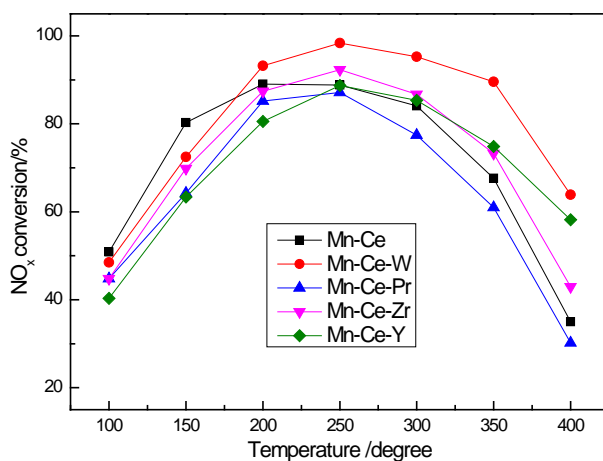


**Figure 4.** NO conversion of Mn-Ce-M (reaction conditions:  $\varphi(\text{NO}) = 1000$  ppm;  $\varphi(\text{NH}_3) = 1200$  ppm;  $\varphi(\text{O}_2) = 5\%$ ;  $\text{N}_2$  as balance;  $\text{GHSV} = 10,000 \text{ h}^{-1}$ ).

catalyst activity only at the high temperature. However, at high temperature range (above  $250^\circ\text{C}$ ), the NO conversions for Mn-Ce-Pr and Mn-Ce-Zr are near to that of Mn-Ce. According to SEM picture, it is possible that uniform particle size and good porosity tends to present good catalyst, especially at low temperature. The reason of the transition metal effect on catalyst performance will be further investigated in the following.

### 3.3. $\text{H}_2$ -TPR Analysis

The doped metal effect on the redox property of Mn-Ce- $\text{M}_{0.025}$  catalysts was observed by  $\text{H}_2$ -TPR, see in **Figure 5**. Use of Mn-Ce catalyst resulted in a broad reduction profile peak in the temperature range of  $163^\circ\text{C} - 486^\circ\text{C}$ ,

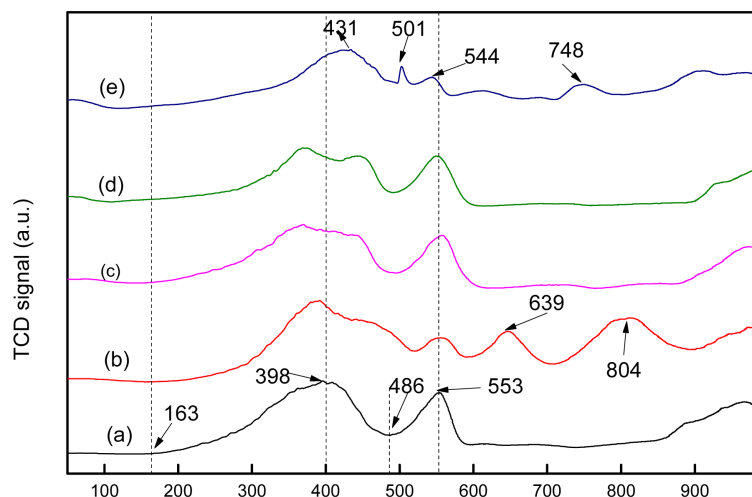


**Figure 5.** H<sub>2</sub>-TPR curves on Mn-Ce-M. (a) Mn-Ce; (b) Mn-Ce-W; (c) Mn-Ce-Pr; (d) Mn-Ce-Zr; (e) Mn-Ce-Y.

which was attributed to the continuous reduction steps of  $\text{MnO}_2 \rightarrow \text{Mn}_2\text{O}_3 \rightarrow \text{Mn}_3\text{O}_4 \rightarrow \text{MnO}$  [7]. The reduction peak at 553°C was attributed to a reduction of  $\text{Ce}^{4+}$  to  $\text{Ce}^{3+}$  on the surface. Above 850°C, the reduction profile peak was from the reduction of  $\text{Ce}^{4+}$  to  $\text{Ce}^{3+}$  in the bulk. When W was introduced to the Mn-Ce catalyst, all reduction peaks were connected together and not back to the baseline. Comparing to Mn-Ce catalyst, the initial reduction temperature of Mn-Ce-W catalyst increased, which may be the reason of its lower catalytic performance at low temperature. On the other hand, the reduction peak area of Mn-Ce-W catalyst at 163°C - 486°C is larger than that for Mn-Ce catalyst. The larger reduction peak area presents the higher oxygen capacity, so the catalytic performance of Mn-Ce-W catalyst begins to exceed that of Mn-Ce catalyst from 200°C. At the same time, the new reduction peaks at 639°C and 804°C can be attributed to tungsten reduction, which result in a greatly increase of reactive oxygen species on the catalyst surface and an improvement of redox ability of the catalyst. Hence, comparing to the Mn-Ce catalyst, the Mn-Ce-W catalyst presents the more excellent catalytic performance. When Pr and Zr element were introduced to the Mn-Ce catalyst, the reduction peak of manganese oxide was divided to two peaks of  $\text{MnO}_2$  or  $\text{Mn}_2\text{O}_3$  reduced to  $\text{Mn}_3\text{O}_4$  below 398°C and  $\text{Mn}_3\text{O}_4$  to  $\text{MnO}$  above 398°C. Two peaks area is lower than that of the Mn-Ce catalyst, which led to lower oxygen capacity. At the same time, the initial reduction temperature of Mn-Ce-Pr and Mn-Ce-Zr catalysts also increased, which indicate low reduction ability at low temperature. These may be two reasons of lower catalytic performance at lower temperature after doping Pr and Zr into the catalyst. At higher temperature, the H<sub>2</sub>-TPR profiles of Mn-Ce, Mn-Ce-Pr and Mn-Ce-Zr is similar, so the NO conversion of Mn-Ce-Pr is small lower to that of Mn-Ce and only a little promotion after doping Zr element to Mn-Ce catalyst. For the Mn-Ce-Y catalyst, two independent peaks present at 431°C and 501°C attributed to manganese oxide, which obviously shift to high temperature and the peaks area is reduced. The reduction peak area of  $\text{Ce}^{4+}$  to  $\text{Ce}^{3+}$  is also reduced that may be due to the action between Y and Ce element. Hence, in Mn-Ce-M catalysts, Mn-Ce-Y behaves the lowest NO conversion at the low temperature (below 250°C). The reduction peak at 748°C can be attributed to  $\text{Y}_2\text{O}_3$ , which promote catalytic performance of Mn-Ce-Y catalyst at high temperature. At 350°C and 400°C, the NO conversion of Mn-Ce-Y is second to that of Mn-Ce-W.

### 3.4. Sulfur Tolerance Analysis

The tolerance to the  $\text{SO}_2$  for these prepared SCR catalysts is further investigated. When  $\text{SO}_2$  concentration is 0.01%, activities of Mn-Ce-M were performed at 250°C, as shown in Figure 6. For all the catalysts, after importing  $\text{SO}_2$  into the reactant gas, the NO conversion is kept or slightly increases within 50 min and then begins to decrease. The performance improvement for the time being can be attributed to the enhancement of  $\text{NH}_3$  adsorption on the acid site formed from the  $\text{SO}_2$  oxidation. After a period of time, a lot of sulfate were formed and adhered to the catalyst surface which leads to catalytic active decrease. Use of Mn-Ce-Pr and Mn-Ce-Y catalysts, the NO conversion are lower than that of Mn-Ce catalyst at initial stage, but decreased slowly and begin to ex-

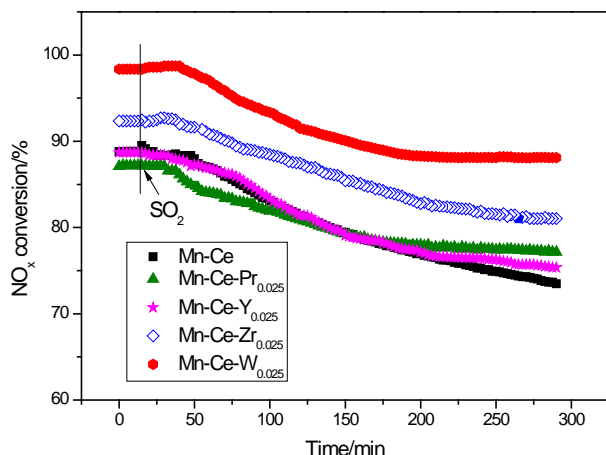


**Figure 6.** SCR activities of Mn-Ce-M<sub>0.025</sub> catalysts in the presence of SO<sub>2</sub> (Reaction conditions:  $\varphi(\text{NO}) = 1000$  ppm;  $\varphi(\text{NH}_3) = 1200$  ppm;  $\varphi(\text{O}_2) = 5\%$ ; N<sub>2</sub> as balance; GHSV = 10,000 h<sup>-1</sup>; SO<sub>2</sub> = 0.01%; reaction temperature = 250°C).

ceed that of Mn-Ce catalyst after 150 min in SO<sub>2</sub> condition. After 275 min in SO<sub>2</sub> condition, the NO<sub>x</sub> conversion decrease from 88.8% to 73.5% over Mn-Ce catalyst, 87.1% to 77.1% over Mn-Ce-Pr catalyst and 88.7% to 75% over Mn-Ce-Y. The results demonstrated that Pr presents better tolerance to the SO<sub>2</sub> than Y element. Doping W and Zr into the Mn-Ce catalyst not only improve the catalytic performance but also enhance the catalyst's sulfur tolerance. In all catalysts, Mn-Ce-W catalyst presented the best performance with 88.1% NO conversion in SO<sub>2</sub> condition after 275 min.

### 3.5. FT-IR Analysis

In order to study the catalyst sulfur tolerance, the fresh catalyst and deactivated Mn-Ce-M catalysts with SO<sub>2</sub> was carried out by FT-IR spectroscopy to detect the adsorbed species on the Mn-Ce-M catalyst. The FTIR spectra for the fresh Mn-Ce catalyst, deactivated Mn-Ce and Mn-Ce-W catalysts with SO<sub>2</sub> deactivated catalysts with SO<sub>2</sub> are shown in Figure 7. The adsorption peak at 1634 cm<sup>-1</sup> band was commonly considered as O-H stretching vibration peak [8]. Comparing to fresh Mn-Ce catalyst, four new bands appeared when the catalysts were exposed to flue gas with SO<sub>2</sub>. NH<sup>4+</sup> was adsorbed on catalyst acid site at 1400 cm<sup>-1</sup> and three bands between 1048 - 1129 cm<sup>-1</sup> were identified as SO<sub>4</sub><sup>2-</sup> adsorption peaks [9] [10]. The results from the FTIR spectra indicated sulfate formation on the catalysts.

There into, the adsorption peak of NH<sup>4+</sup> was weakest on Mn-Ce catalyst, but the strongest SO<sub>4</sub><sup>2-</sup> peaks were formed. That is to say, over Mn-Ce catalyst, a little ammonium sulfate or ammonium bisulfate was formed, but a lot of metal sulphates deposited. So, the maximum sulfate formation was observed on Mn-Ce catalyst, which may be the main reason of the catalyst inactivation. Metal doping into the Mn-Ce catalyst could inhibit the sulfate formation, especially the suppression to the deposition of metal sulfate, which could lead to the block of catalyst pores or channels. The weakest SO<sub>4</sub><sup>2-</sup> peaks presented over Mn-Ce-W catalyst, which proved that W addition could greatly inhibit the sulfate formation. Then Mn-Ce-W catalyst presented the optimal performance in the aspect of sulfur tolerance.

## 4. Conclusion

Mn-based catalysts were prepared via ultrasonic immersing method for the selective catalytic reduction (SCR) of NO<sub>x</sub> from fuel gas. Transition metals effect on the Catalysts' DeNO<sub>x</sub> efficiency and tolerance to sulfur were investigated. SEM and XRD results demonstrate metal elements high dispersion on TiO<sub>2</sub> and uniform particle size about 500 nm to 800 nm. Sulfur tolerance analysis indicated that transition metals M can improve the catalysts' performance when SO<sub>2</sub> exists in the fuel gas. Mn-Ce-W catalyst performs the best NO<sub>x</sub> conversion of 93.2% at 200°C and 98.4% at 250°C, respectively. From the FTIR results, the weakest SO<sub>4</sub><sup>2-</sup> peak over the Mn-Ce-W catalyst which proved W element inhibit sulfate formation, especially metal sulfate, and this is the reason of good sulfur tolerance for the catalysts.

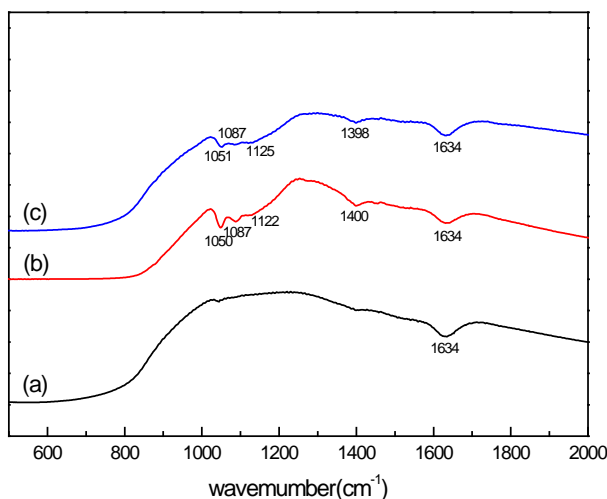


**Figure 7.** FT-IR spectra of fresh and deactivated catalysts with SO<sub>2</sub>. (a) Fresh Mn-Ce; (b) deactivated Mn-Ce catalysts; (c) deactivated Mn-Ce-W<sub>0.025</sub> catalysts.

## Acknowledgements

We acknowledge the support of the National Support Plan (2011BAA04B07) and Beijing Institute of Technology Basic Research Fund (20111042014).

## References

- [1] Qi, G., Yang, R.T. and Chang, R. (2004) MnO<sub>x</sub>-CeO<sub>2</sub> Mixed Oxides Prepared by Co-Precipitation for Selective Catalytic Reduction of NO with NH<sub>3</sub> at Low Temperatures. *Applied Catalysis B*, **51**, 93-106. <http://dx.doi.org/10.1016/j.apcatb.2004.01.023>
- [2] Carja, G., Kameshima, Y., Okada, K., *et al.* (2007) Mn-Ce/ZSM5 as a New Superior Catalyst for NO Reduction with NH<sub>3</sub>. *Applied Catalysis B*, **73**, 60-64. <http://dx.doi.org/10.1016/j.apcatb.2006.06.003>
- [3] Tang, X.L., Hao, J.M., Yi, H.H., *et al.* (2007) Low-Temperature SCR of NO with NH<sub>3</sub> over AC/C Supported Manganese-Based Monolithic Catalysts. *Catalysis Today*, **126**, 406-411. <http://dx.doi.org/10.1016/j.cattod.2007.06.013>
- [4] Wu, Z.B., Jin, R.B., Liu, Y. and Wang, H.Q. (2008) Ceria Modified MnO<sub>x</sub>/TiO<sub>2</sub> as a Superior Catalyst for NO Reduction with NH<sub>3</sub> at Low-Temperature. *Catalysis Communications*, **9**, 2217-2220.
- [5] Uddin, A.M., Ishibe, K., *et al.* (2007) Effects of SO<sub>2</sub> on NO Adsorption and NO<sub>2</sub> Formation over TiO<sub>2</sub> Low-Temperature SCR Catalyst. *Industrial & Engineering Chemistry Research*, **46**, 1672.
- [6] Wu, D.W., Zhang, Q.L., Lin, T., *et al.* (2011) Ce<sub>x</sub>Ti<sub>1-x</sub>O<sub>2</sub> Supported Manganese-Based Catalyst: Preparation and Catalytic Performance for Selective Reduction of NO with NH<sub>3</sub> at Lower Temperature. *Chinese Journal of Inorganic Chemistry*, **27**, 53.
- [7] Maitarad, P., Zhang, D.S., Gao, R.H., *et al.* (2013) Combination of Experimental and Theoretical Investigations of MnO<sub>x</sub>/Ce<sub>0.9</sub>Zr<sub>0.1</sub>O<sub>2</sub> Nanorods for Selective Catalytic Reduction of NO with Ammonia. *Journal of Physical Chemistry C*, **117**, 9999-10006. <http://dx.doi.org/10.1021/jp400504m>
- [8] Othman, I, Mohamed, R.M. and Ibrahim, F.M. (2007) Study of Photocatalytic Oxidation of Indigo Carmine Dye on Mn-Supported TiO<sub>2</sub>. *Journal of Photochemistry and Photobiology A: Chemistry*, **189**, 82-83. <http://dx.doi.org/10.1016/j.jphotochem.2007.01.010>
- [9] Topsoe, N.Y. (1994) Mechanism of the Selective Catalytic Reduction of Nitric Oxide by Ammonia Elucidated by in Situ On-Line Fourier Transform Infrared Spectroscopy. *Science*, **265**, 1217-1219. <http://dx.doi.org/10.1126/science.265.5176.1217>
- [10] Wu, Z., Jiang, B., Liu, Y., Wang, H. and Jin, R. (2007) DRIFT Study of Manganese/Titania-Based Catalysts for Low-Temperature Selective Catalytic Reduction of NO with NH<sub>3</sub>. *Environmental Science and Technology Journal*, **41**, 5812-5817. <http://dx.doi.org/10.1021/es0700350>

Scientific Research Publishing (SCIRP) is one of the largest Open Access journal publishers. It is currently publishing more than 200 open access, online, peer-reviewed journals covering a wide range of academic disciplines. SCIRP serves the worldwide academic communities and contributes to the progress and application of science with its publication.

Other selected journals from SCIRP are listed as below. Submit your manuscript to us via either [submit@scirp.org](mailto:submit@scirp.org) or **Online Submission Portal**.

